Taylor & Francis
Taylor & Francis Group

Automatika
Journal for Control, Measurement, Electronics, Computing and Communications

ISSN: (Print) (Online) Journal homepage: https://www.tandfonline.com/loi/taut20

A Laguerre spectral method for quadratic optimal control of nonlinear systems in a semi-infinite interval

Mojtaba Masoumnezhad , Mohammadhossein Saeedi , Haijun Yu & Hassan Saberi Nik

To cite this article: Mojtaba Masoumnezhad , Mohammadhossein Saeedi , Haijun Yu & Hassan Saberi Nik (2020) A Laguerre spectral method for quadratic optimal control of nonlinear systems in a semi-infinite interval, Automatika, 61:3, 461-474, DOI: 10.1080/00051144.2020.1774724

To link to this article: https://doi.org/10.1080/00051144.2020.1774724

Published online: 16 Jun 2020.

AUTOMATIKA
2020, VOL. 61, NO. 3, 461–474
https://doi.org/10.1080/00051144.2020.1774724

REGULAR PAPER

OPEN ACCESS Check for updates

A Laguerre spectral method for quadratic optimal control of nonlinear systems in a semi-infinite interval

Mojtaba Masoumnezhad[a], Mohammadhossein Saeedi[b], Haijun Yu[c,d] and Hassan Saberi Nik[e]

[a]Department of Mechanical Engineering, Faculty of Chamran, Guilan Branch, Technical and Vocational University (TVU), Tehran, Iran; [b]Department of Industrial, Manufacturing and Systems Engineering, Texas Tech University, Lubbock, TX, USA; [c]School of Mathematical Sciences, University of Chinese Academy of Sciences, Beijing, People's Republic of China; [d]Academy of Mathematics and Systems Science, Beijing, People's Republic of China; [e]Department of Mathematics, Neyshabur Branch, Islamic Azad University, Neyshabur, Iran

ABSTRACT
This paper presents a Laguerre homotopy method for quadratic optimal control problems in semi-infinite intervals (LaHOC), with particular interests given to nonlinear interconnected large-scale dynamic systems. In LaHOC, the spectral homotopy analysis method is used to derive an iterative solver for the nonlinear two-point boundary value problem derived from Pontryagin's maximum principle. A proof of local convergence of the LaHOC is provided. Numerical comparisons are made between the LaHOC, Matlab BVP5C generated results and results from the literature for two nonlinear optimal control problems. The results show that LaHOC is superior in both accuracy and efficiency.

ARTICLE HISTORY
Received 13 June 2020
Accepted 17 April 2020

KEYWORDS
Laguerre method; collocation method; optimal control problems; spectral homotopy analysis method (SHAM); semi-infinite interval

1. Introduction

Large-scale systems are found in many practical applications, such as power systems and physical plants. During the past several years, the problem of analysis and synthesis for dynamic large-scale systems has received considerable attention. Based on the characteristics of large-scale systems, many results have been proposed, such as modelling, stability, robust control, decentralized, and so on [1–6].

The optimal control of nonlinear large-scale systems has been widely investigated in recent decades. For instance, a new successive approximation approach (SAA) was proposed in [7]. In this approach, instead of directly solving the nonlinear large-scale two-point boundary value problem (TPBVP), derived from the maximum principle, a sequence of non-homogeneous linear time-varying TPBVPs is solved iteratively. Also, in [8] a new technique, called the modal series method, has been extended to solve a class of infinite horizon OCPs of nonlinear interconnected large-scale dynamic systems, where the cost function is assumed to be quadratic and decoupled. This method provides the solution of autonomous nonlinear systems in terms of fundamental and interacting modes. Conventional methods of optimal control are generally impractical for many nonlinear large-scale systems because of the dimensionality problem and high complexity in calculations. One example is the state-dependent Riccati equation (SDRE) method [9]. Although this scheme has been widely used in many applications, its major limitation is that it needs to solve a sequence of matrix Riccati algebraic equations at each sample state along the trajectory. This property may take a long computing time and large memory space. Therefore, developing new methods is necessary for solving nonlinear large-scale optimal control problems (OCPs) [10].

The use of spectral methods for optimal control problems usually leads to a more efficient method than finite element or finite difference approaches. Chebyshev's and Legendre's methods are commonly used for problems in finite intervals [11,12]. For infinite or semi-infinite intervals, there are several choices for the approximation bases: Hermite polynomials/functions [13], Laguerre polynomials/functions [14], mapped Jacobi bases [15–17]. Furthermore, one class of very important applications of OCP in unbounded intervals is the so-called Minimum Action Method (MAM) [18] used in finding the most probable transition path in phase transition phenomena. Using MAM to study spatial extended transitions, such as fluid instability transition, is usually equivalent to solve a large-scale nonlinear optimal control problem [18].

The homotopy analysis method is an analytical technique for solving nonlinear differential equations. The HAM [19,20] was first proposed by Liao in 1992 to solve lots of nonlinear problems. This method has been successfully applied to many nonlinear problems, such as physical models with an infinite number of singularities [21], nonlinear eigenvalue problems [22], fractional Sturm–Liouville problems [23], optimal control

CONTACT Hassan Saberi Nik saberi_hssn@yahoo.com

problems [24,25], Cahn–Hilliard initial value problem [26], semi-linear elliptic boundary value problems [27] and so on [28]. The HAM contains a certain auxiliary parameter $\hbar$ which provides us with a simple way to adjust and control the convergence region and rate of convergence of the series solution. Moreover, by means of the so-called $\hbar$-curve, it is easy to determine the valid regions of $\hbar$ to gain a convergent series solution. The HAM, however, suffers from a number of restrictive measures, such as the requirement that the solution sought ought to conform to the so-called rule of solution expression and the rule of coefficient ergodicity. These HAM requirements are meant to ensure that the implementation of the method results in a series of differential equations can be solved analytically.

Recently, Motsa et al. [29–32] proposed a spectral modification of the homotopy analysis method, the spectral-homotopy analysis method (SHAM). The SHAM approach imports some of the ideas of the HAM such as the use of the convergence controlling auxiliary parameter. In the implementation of the SHAM, the sequence of the so-called deformation differential equations is converted into a matrix system by applying the Chebyshev or Legendre pseudospectral method [31]. But so far, to our knowledge, there is no work concerning the combination of Laguerre polynomials [33] with the HAM. This paper presents a spectral homotopy analysis method based on modified Laguerre–Radau interpolation to solve nonlinear large-scale optimal control problems (OCPs). This process has several advantages. First, it possesses spectral accuracy [34,35]. Next, it is easier to be implemented, especially for nonlinear systems. Furthermore, it is applicable to long-time calculations.

The paper is organized as follows. The nonlinear interconnected OCP and optimality conditions are described in Section 2. In Section 3, we propose the new algorithm by using the modified Laguerre polynomials. The convergence of the proposed method is proved in Section 4. We present the numerical results in Section 5, which demonstrate the spectral accuracy of the proposed methods. The final section is for concluding remarks.

2. The nonlinear interconnected OCP

Consider a nonlinear interconnected large-scale dynamic system which can be decomposed into N interconnected subsystems. The ith subsystem for $i = 1, 2, \dots, N$ is described by

$$\begin{aligned}&\dot{x}_i(t) = A_i x_i(t) + B_i u_i(t) + f_i(x(t)), \quad t > t_0,\\ &x_i(t_0) = x_{i_0},\end{aligned} \tag{1}$$

with $x_i \in \mathbb{R}^{n_i}$ denoting the state vector, $u_i \in \mathbb{R}^{m_i}$ the control vector of the ith subsystem, respectively, $x = (x_1^T, x_2^T, \dots x_N^T)^T$, $\sum_{i=1}^{N} n_i = n$, $F_i : \mathbb{R}^n \to \mathbb{R}^{n_i}$ is a nonlinear analytic vector function where $F_i(0) = 0$, and $x_{i_0} \in \mathbb{R}^{n_i}$ is the initial state vector. Also, A_i and B_i are constant matrices of appropriate dimensions such that the pair (A_i, B_i) is completely controllable [8]. Furthermore, the infinite horizon quadratic cost function to be minimized is given by

$$J = \frac{1}{2}\sum_{i=1}^{N}\left\{\int_{t_0}^{\infty}(x_i^T(t)Qx_i(t) + u_i^T(t)R_iu_i(t))\mathrm{d}t\right\}, \tag{2}$$

where $Q_i \in \mathbb{R}^{n_i\times n_i}$ and $R_i \in \mathbb{R}^{m_i\times m_i}$ are positive semidefinite and positive definite matrices, respectively. Note that quadratic cost function (2) is assumed to be decoupled as a superposition of the cost functions of the subsystems.

According to Pontryagin's maximum principle, the optimality conditions are obtained as the following nonlinear TPBVP:

$$\begin{aligned}&\dot{x}_i(t) = A_i x_i(t) - B_i R_i^{-1} B_i^T \lambda_i(t) + f_i(x(t)), \quad t > t_0,\\ &\dot{\lambda}_i(t) = -Q_i x_i(t) - A_i^T \lambda_i(t)\\ &\qquad - \Psi_i(x(t), \lambda(t)), \quad t > t_0,\\ &x_i(t_0) = x_{i_0}, \lambda_i(\infty) = 0,\\ &\quad i = 1, 2, \dots, N,\end{aligned} \tag{3}$$

where $\lambda_i(t) \in \mathbb{R}^{n_i}$ is the co-state vector, $\lambda = (\lambda_1^T, \lambda_2^T, \dots \lambda_N^T)^T$, and $\Psi_i(x(t), \lambda(t)) = \sum_{j=1}^{N}(\partial f_j(x(t))/\partial x_i(t))\lambda_j(t)$. Also the optimal control law of the ith subsystem is given by

$$u_i^*(t) = -R_i^{-1} B_i^T \lambda_i(t), \quad t > t_0, \quad i = 1, 2, \dots N. \tag{4}$$

Unfortunately, problem (3) is a nonlinear large-scale TPBVP which is decomposed into N interconnected subproblems. In general, it is extremely difficult to solve this problem analytically or even numerically, except in a few simple cases. In order to overcome this difficulty, we will present the LaHOC method in the next section.

3. Laguerre polynomials and spectral homotopy analysis method

In this section, we give a brief description of the basic idea of the Laguerre homotopy method for solving nonlinear boundary value problems. At first, we take into account the following properties of the modified Laguerre polynomials.

3.1. *Properties of the modified Laguerre polynomials*

Let $\omega_\beta(t) = e^{-\beta t}$, $\beta > 0$, and define the weighted space $L^2_{\omega_\beta}(0, \infty)$ as usual, with the following inner product and norm [14]:

$$(u,v)_{\omega_\beta} = \int_0^\infty u(t)v(t)\omega_\beta(t)\,\mathrm{d}t, \quad ||v||_{\omega_\beta} = (v,v)_{\omega_\beta}. \tag{5}$$

The modified Laguerre polynomial of degree l is defined by

$$\mathcal{L}_l^\beta(t) = \frac{1}{l!}e^{\beta t}\frac{\mathrm{d}^l}{\mathrm{d}t^l}(t^l e^{-\beta t}), \quad l \geq 0. \tag{6}$$

They satisfy the recurrence relation

$$\frac{\mathrm{d}}{\mathrm{d}t}\mathcal{L}_l^\beta(t) = \frac{\mathrm{d}}{\mathrm{d}t}\mathcal{L}_{l-1}^\beta(t) - \beta\mathcal{L}_{l-1}^\beta(t), \quad l \geq 1. \tag{7}$$

The set of Laguerre polynomials is a complete $L^2_{\omega_\beta}(0,\infty)$-orthogonal system, namely,

$$(\mathcal{L}_l^\beta, \mathcal{L}_m^\beta)_{\omega_\beta} = \frac{1}{\beta}\delta_{l,m}, \tag{8}$$

where $\delta_{l,m}$ is the Kronecker symbol. Thus, for any $v \in L^2_{\omega_\beta}(0,\infty)$,

$$v(t) = \sum_{j=0}^{\infty} \hat{v}_l \mathcal{L}_l^\beta(t), \tag{9}$$

where the coefficients $\hat{v}_l$ are given by

$$\hat{v}_l = \beta(v, \mathcal{L}_l^\beta)_{\omega_\beta}. \tag{10}$$

Now, let N be any positive integer, and $\mathcal{P}_N(0,\infty)$ the set of all algebraic polynomials of degree at most N. We denote by $t^N_{\beta,j}$, $0 \leq j \leq N$, the nodes of modified Laguerre–Radau interpolation. Indeed, $t^N_{\beta,0} = 0$ and $t^N_{\beta,j}$, $1 \leq j \leq N$, are the distinct zeros of $(\mathrm{d}/\mathrm{d}t)\mathcal{L}^\beta_{N+1}(t)$. By using (7), the corresponding Christoffel numbers are as follows:

$$\begin{aligned} \omega^N_{\beta,0} &= \frac{1}{\beta(N+1)}, \\ \omega^N_{\beta,j} &= \frac{1}{\beta(N+1)\mathcal{L}^\beta_N(t^N_{\beta,j})\ \mathcal{L}^\beta_{N+1}(t^N_{\beta,j})}. \end{aligned} \tag{11}$$

For any $\Phi \in \mathcal{P}_{2N}(0,\infty)$,

$$\sum_{j=0}^{N} \Phi(t^N_{\beta,j})\omega^N_{\beta,j} = \int_0^\infty \Phi(t)\omega_\beta(t)\,\mathrm{d}t. \tag{12}$$

Next, we define the following discrete inner product and norm,

$$\begin{aligned} (u,v)_{\omega_\beta,N} &= \sum_{j=0}^{N} u(t^N_{\beta,j})v(t^N_{\beta,j})\omega^N_{\beta,j}, \\ ||v||_{\omega_\beta,N} &= (v,v)^{12}_{\omega_\beta,N}. \end{aligned} \tag{13}$$

For any $\Phi, \psi \in \mathcal{P}_N(0,\infty)$,

$$(\Phi,\psi)_{\omega_\beta} = (\Phi,\psi)_{\omega_\beta,N}, \quad ||v||_{\omega_\beta} = ||v||_{\omega_\beta,N}. \tag{14}$$

3.2. Spectral homotopy analysis method

In this section, we give a description of the SHAM with the Laguerre polynomials basis. This will be followed by a description of the new version of the SHAM algorithm [29]. To this end, consider a general n-dimensional initial value problem described as

$$\dot{\mathbf{z}}(t) = \mathbf{f}(t, \mathbf{z}(t)), \quad \mathbf{z}(t_0) = \mathbf{z}^0, \tag{15}$$

$$\mathbf{z}: \mathbb{R} \to \mathbb{R}^n, \quad \mathbf{f}: \mathbb{R}\times\mathbb{R}^n \to \mathbb{R}^n. \tag{16}$$

We make the usual assumption that $\mathbf{f}$ is sufficiently smooth for linearization techniques to be valid. If $\mathbf{z} = (z_1, z_2, \ldots, z_n)$, we can apply the SHAM by rewriting Equation (15) as

$$\dot{z}_r + \sum_{k=1}^{n} \sigma_{r,k} z_k + g_r(z_1, z_2, \ldots, z_n) = 0, \tag{17}$$

subject to the initial conditions

$$z_r(0) = z_r^0, \tag{18}$$

where z_r^0 are the given initial conditions, $\sigma_{r,k}$ are known constant parameters and g_r is the nonlinear component of the rth equation.

The SHAM approach imports the conventional ideas of the standard homotopy analysis method by defining the following zeroth-order deformation equations:

$$(1-q)\mathcal{L}_r\left[\tilde{z}_r(t;q) - z_{r,0}(t)\right] = q\hbar_r\mathcal{N}_r[\tilde{\mathbf{z}}(t;q)], \tag{19}$$

where $q \in [0,1]$ is an embedding parameter, $\tilde{z}_r(t;q)$ are unknown functions, and $\hbar_r$ is a convergence controlling parameter. The operators $\mathcal{L}_r$ and $\mathcal{N}_r$ are defined as

$$\mathcal{L}_r[\tilde{z}_r(t;q)] = \frac{\partial \tilde{z}_r}{\partial t} + \sum_{k=1}^{n}\sigma_{r,k}\tilde{z}_k, \tag{20}$$

$$\begin{aligned} \mathcal{N}_r[\tilde{\mathbf{z}}(t;q)] &= \mathcal{L}_r[\tilde{z}_r(t;q)] \\ &\quad + g_r[\tilde{z}_1(t;q), \tilde{z}_2(t;q), \ldots, \tilde{z}_n(t;q)]. \end{aligned} \tag{21}$$

Using the ideas of the standard HAM approach [20], we differentiate zeroth-order Equations (19) m times with respect to q and then set $q = 0$ and finally divide the resulting equations by $m!$ to obtain the following equations, which are referred to as the mth order (or higher order) deformation equations:

$$\mathcal{L}_r[z_{r,m}(t) - \chi_m z_{r,m-1}(t)] = \hbar_r R_{r,m-1}, \quad m \geq 1, \tag{22}$$

subject to

$$z_{r,m}(0) = 0, \tag{23}$$

where

$$R_{r,m-1} = \frac{1}{(m-1)!}\left.\frac{\partial^{m-1}\mathcal{N}_r[\tilde{\mathbf{z}}(t;q)]}{\partial q^{m-1}}\right|_{q=0} \tag{24}$$

and

$$\chi_m = \begin{cases} 0, & m \leqslant 1, \\ 1, & m > 1. \end{cases} \tag{25}$$

After obtaining solutions for Equation (22), the approximate solution for each $z_r(t)$ is determined as the series solution

$$z_r(t) = z_{r,0}(t) + z_{r,1}(t) + z_{r,2}(t) + \dots \tag{26}$$

A HAM solution is said to be of order M if the above series is truncated at $m = M$, that is, if

$$z_r(t) = \sum_{m=0}^{M} z_{r,m}(t). \tag{27}$$

A suitable initial guess to start off the SHAM algorithm is obtained by solving the linear part of (17) subject to the given initial conditions, that is, we solve

$$\mathcal{L}_r[z_{r,0}(t)] = \phi_r(t), \quad z_{r,0}(0) = z_r^0. \tag{28}$$

If Equation (28) cannot be solved exactly, the spectral collocation method is used as a means of solution. The solution $z_{r,0}(t)$ of Equation (28) is then fed to (22) which is iteratively solved for $z_{r,m}(t)$ (for $m = 1, 2, 3, \dots, M$).

In this paper, we use the Laguerre pseudo-spectral method to solve Equations (22)–(24). The pseudo-spectral derivative $D_N(z)$ of a continuous function z is defined by

$$D_N(z) = D[I_N(z)], \tag{29}$$

that is, $D_N(z)$ is the derivative of the interpolating polynomial of z. Moreover, D_N can be expressed in terms of a matrix, the pseudo-spectral derivation matrix D_β:

$$D_\beta = [(d_\beta)_{ij}]_{i,j=0,1,\dots,N}.$$

Indeed, given the nodes $\{x_j^{(\beta)}\}_{j=0}^N$, an approximation $z \in \mathcal{P}_N^{(\beta)}$ of an unknown function and $\{(h_\beta)_j\}$, the Lagrange interpolation polynomials associated with the points x_j, differentiating m times the expression

$$z_\beta(x) = \sum_{j=0}^{N} z_\beta(x_j)(h_\beta)_j(x)$$

yields:

$$z_\beta^{(m)}(x_k) = \sum_{j=0}^{N} (h_\beta)_j^{(m)}(x_k) z_\beta(x_j), \quad 0 \le k \le N.$$

If we define

$$z_\beta^{(m)} = \left(z_\beta^{(m)}(x_0), z_\beta^{(m)}(x_1), \dots, z_\beta^{(m)}(x_N)\right)^T,$$

$$z_\beta = z_\beta^{(0)},$$

$$D_\beta^{(m)} = \left[(d_\beta)_{ij}^{(m)} = (h_\beta)_j^{(m)}(x_i)\right]_{0\le i,j\le N},$$

$$(d_\beta)_{ij}^{(m)} = (h_\beta)_j^{(m)}(x_i),$$

then

$$D_\beta = D_\beta^{(1)}, (d_\beta)_{ij} = (d_\beta)_{ij}^{(1)}.$$

We now state two important results. The first ensures that it is sufficient to compute the first-order differentiation matrix, and the second gives the general expression of its entries.

Lemma 3.1 ([33]):

$$D_\beta^{(m)} = D_\beta . D_\beta \cdots D_\beta = D_\beta^m, \quad m \ge 1. \tag{30}$$

Let $\{x_j^{(\beta)}\}_{j=0}^N$ be the Gauss–Laguerre (GL) or Gauss–Laguerre–Radau (GLR) nodes and $z \in \mathcal{P}_N^{(\beta)}$. Let $\{(h_\beta)_j(x)\}_{j=0}^N$ be the Lagrange interpolation polynomials relative to $\{x_j^{(\beta)}\}_{j=0}^N$. From Lemma 3.1, we have

$$z_\beta^{(m)} = D_\beta^m z_\beta, \quad m \ge 1.$$

Next we have:

Lemma 3.2 ([33]): *The entries of the differentiation matrix D_β associated with the GL and GLR points $\{x_j^{(\beta)}\}_{j=0}^N$ have the following form:*

- *GL points: $\{x_j^{(\beta)}\}_{j=0}^N$ are the zeros of $\mathscr{L}_{N+1}^{(\beta)}(x)$,*

$$d_{ij} = \begin{cases} \dfrac{\mathscr{L}_N^{(\beta)}\left(x_i^{(\beta)}\right)}{\left(x_i^{(\beta)} - x_j^{(\beta)}\right)\mathscr{L}_N^{(\beta)}\left(x_j^{(\beta)}\right)} & \text{if } i \neq j, \\ \dfrac{\beta x_i^{(\beta)} - N - 2}{2x_i^{(\beta)}} & \text{if } i = j, \end{cases} \tag{31}$$

- *GLR points: $x_0 = 0$, $\{x_j^{(\beta)}\}_{j=1}^N$ are the zeros of $\frac{\partial}{\partial x}\mathscr{L}_{N+1}^{(\beta)}(x)$,*

$$d_{ij} = \begin{cases} \dfrac{\mathscr{L}_{N+1}^{(\beta)}\left(x_i^{(\beta)}\right)}{\left(x_i^{(\beta)} - x_j^{(\beta)}\right)\mathscr{L}_{N+1}^{(\beta)}\left(x_j^{(\beta)}\right)} & \text{if } i \neq j, \\ \dfrac{\beta}{2} & \text{if } i = j \neq 0, \\ \dfrac{-\beta N}{2} & \text{if } i = j = 0. \end{cases} \tag{32}$$

Applying the Laguerre spectral collocation method in Equations (22)–(24) gives

$$\mathbf{A}\,[\mathbf{W}_m - \chi_m \mathbf{W}_{m-1}] = \hbar_r \mathbf{R}_{m-1}, \quad \mathbf{W}_m(\tau_0) = 0, \quad \mathbf{W}_m(\tau_N) = 0, \tag{33}$$

where $\mathbf{R}_{m-1}$ is an $(N+1)n \times 1$ vector corresponding to $R_{r,m-1}$ when evaluated at the collocation points and $\mathbf{W}_m = [\tilde{\mathbf{z}}_{1,m}; \tilde{\mathbf{z}}_{2,m}; \ldots; \tilde{\mathbf{z}}_{n,m}]$.

The matrix $\mathbf{A}$ is an $(N+1)n \times (N+1)n$ matrix that is derived from transforming the linear operator $\mathcal{L}_r$ using the derivative matrix D_β (we omit subscript β for simplicity) and is defined as

$$\mathbf{A} = \begin{bmatrix} A_{11} & A_{12} & \cdots & A_{1n} \\ A_{21} & A_{22} & \cdots & A_{2n} \\ \vdots & & \ddots & \vdots \\ A_{n1} & A_{n2} & \cdots & A_{nn} \end{bmatrix}, \quad \text{with}$$

$$\mathbf{A}_{pq} = \begin{cases} \mathbf{D} + \sigma_{pq}\mathbf{I}, & p = q, \\ \sigma_{pq}\mathbf{I}, & p \neq q, \end{cases} \tag{34}$$

where $\mathbf{I}$ is an identity matrix of order $N+1$.

Thus, starting from the initial approximation, recurrence formula (33) can be used to obtain the solution $z_r(t)$.

4. Convergence analysis of LaHOC

To analyse the convergence of LaHOC, we first recall the mth order (or higher order) deformation equation

$$\mathcal{L}[z_m(t) - \chi_m z_{m-1}(t)] = \hbar H(t) R_{m-1}, \tag{35}$$

subject to the initial condition

$$z_{m,1:n}(t_0) = 0, \tag{36}$$

where $H(t) \neq 0$ is an auxiliary function,

$$R_{m-1} = \mathcal{L}[z_{m-1}] + \mathcal{N}_{m-1}[z_0, z_1, \ldots, z_{m-1}] - (1 - \chi_m)\phi(t), \tag{37}$$

where $z_{r,m}$, $\mathcal{L}_r$ and $\mathcal{N}_r$ in (22) are the rth components of z_{m-1} and operators $\mathcal{L}$ and $\mathcal{N}$, respectively. Let us define the nonlinear operator $\mathcal{N}$ and the sequence $\{Z_m\}_{m=0}^{\infty}$ as

$$\mathcal{N}[\mathbf{z}(t)] = \sum_{k=0}^{\infty} N_k(z_0, z_1, \ldots, z_k), \tag{38}$$

$$\begin{cases} Z_0 = z_0, \\ Z_1 = z_0 + z_1, \\ \vdots \\ Z_m = z_0 + z_1 + z_2 + \cdots + z_m. \end{cases} \tag{39}$$

Therefore, we have

$$\mathcal{L}[z_m(t)] = \hbar H(t) \left\{ \sum_{k=0}^{m-1} \mathcal{L}[z_k] + \sum_{k=0}^{m-1} \mathcal{N}_k - \phi(t) \right\}, \tag{40}$$

from (39) we have

$$\mathcal{L}[Z_m(t) - Z_{m-1}(t)] = \hbar H(t)\{\mathcal{L}[Z_{m-1}] + \mathcal{N}[Z_{m-1}] - \phi(t)\}, \tag{41}$$

subject to the initial condition

$$Z_{m,1:n}(t_0) = 0. \tag{42}$$

Consequently, the collocation method is based on a solution $Z^N(t) \in \mathcal{P}_{N+1}(0,\infty)$, for (41) such that

$$\begin{aligned} &\mathcal{L}[Z_m^N(t_{\beta,k}^N) - Z_{m-1}^N(t_{\beta,k}^N)] \\ &\quad = \hbar H^N(t_{\beta,k}^N)\{\mathcal{L}[Z_{m-1}^N(t_{\beta,k}^N)] + \mathcal{N}[Z_{m-1}^N(t_{\beta,k}^N)] \\ &\quad - \phi^N(t_{\beta,k}^N)\}, \end{aligned} \tag{43}$$

subject to the initial condition

$$Z_{m,1:n}^N(t_0) = 0. \tag{44}$$

From (43), we have

$$\begin{aligned} \mathcal{L}[Z_m^N(t_{\beta,k}^N)] &= (1 + \hbar H^N(t_{\beta,k}^N))\mathcal{L}[Z_{m-1}^N(t_{\beta,k}^N)] \\ &\quad + \hbar H^N(t_{\beta,k}^N)\{\mathcal{N}[Z_{m-1}^N(t_{\beta,k}^N)] \\ &\quad - \phi^N(t_{\beta,k}^N)\}, \quad \leq k \leq N, \quad m \geq 1, \\ Z_{m,1:n}^N(t_0) &= 0, \quad m \geq 0. \end{aligned} \tag{45}$$

Now, we choose $L[Z(t)] = (\mathrm{d}/\mathrm{d}t)Z + \alpha(t)Z$, $N[Z(t)] = -\alpha(t)Z - f(t,Z)$ and $\phi(t) \equiv 0$, where $\alpha(t)$ is an arbitrary analytic function.

Let $\tilde{Z}_m^N(t) = Z_m^N(t) - Z_{m-1}^N(t)$, then we have from (45) that

$$\begin{aligned} \mathcal{L}[\tilde{Z}_m^N(t_{\beta,k}^N)] &= (1 + \hbar H(t_{\beta,k}^N))\mathcal{L}[Z_{m-1}^N(t_{\beta,k}^N) \\ &\quad - Z_{m-2}^N(t_{\beta,k}^N)] + \hbar H(t_{T,k}^N) \\ &\quad \times \{\mathcal{N}[Z_{m-1}^N(t_{\beta,k}^N)] - \mathcal{N}[Z_{m-2}^N(t_{\beta,k}^N)]\}, \\ &\quad 0 \leq k \leq N, \quad m \geq 1, \end{aligned} \tag{46}$$

or according to the definitions of $L[Z(t)]$ and $N[Z(t)]$,

$$\begin{aligned} &\frac{\mathrm{d}}{\mathrm{d}t}[\tilde{Z}_m^N(t_{\beta,k}^N)] + \alpha(t_{\beta,k}^N)\tilde{Z}_m^N \\ &\quad = (1 + \hbar H(t_{\beta,k}^N))\frac{\mathrm{d}}{\mathrm{d}t}[\tilde{Z}_{m-1}^N(t_{\beta,k}^N)] + \alpha(t_{\beta,k}^N)\tilde{Z}_{m-1}^N \\ &\quad \times \hbar H(t_{\beta,k}^N)\{f(t_{\beta,k}^N, Z_{m-1}^N(t_{\beta,k}^N)) \\ &\quad - f(t_{\beta,k}^N, Z_{m-2}^N(t_{\beta,k}^N))\}, \quad 0 \leq k \leq N, \quad m \geq 1, \end{aligned} \tag{47}$$

Theorem 4.1: *Assume that for any $k = 0, 1, \ldots, N$, $\mathscr{Z}_k = \{Z_m^N(t_{\beta,k}^N)\}_0^{\infty}$ is the LaHOC sequence produced by (45). Furthermore, assume $\alpha_0 = \min_{t\in[0,\infty)} \alpha(t)$, $\alpha_1 = \max_{t\in[0,\infty)} |\alpha(t)|$ and $H = \max_{t\in[0,\infty)} |H(t)|$ and*

$$\|f(\cdot, Z_m^N) - f(\cdot, Z_{m-1}^N)\|_{\omega_\beta,N} \leq L_f \|Z_m^N - Z_{m-1}^N\|_{\omega_\beta,N}, \tag{48}$$

for some constant $L_f > 0$. Then for any initial n-vector $Z_0^N(t_{\beta,k}^N)$, $\mathscr{Z}_k$ converges to some $\hat{Z}(t_{\beta,k}^N)$ which is the exact *solution of* (17), *at any GLR point*, $t^N_{\beta,k}$, *if*

$$\gamma = \frac{N|1+\hbar H| + \alpha_1 + |\hbar| H L_f}{\beta/2+\alpha_0} < 1. \quad (49)$$

Proof: 1. Using (5) and integrating by parts yield that

$$\left(\tilde{Z}^N_m, \frac{\mathrm{d}}{\mathrm{d}t}\tilde{Z}^N_m\right)_{\omega_\beta,N} = \left(\tilde{Z}^N_m, \frac{\mathrm{d}}{\mathrm{d}t}\tilde{Z}^N_m\right)_{\omega_\beta} = \frac{1}{2}\left[e^{-\beta t}(\tilde{Z}^N_m)^2 \,|_0^\infty + \int_0^\infty \beta e^{-\beta t}(\tilde{Z}^N_m)^2 \,\mathrm{d}t\right], \quad (50)$$

then we have

$$2\left(\tilde{Z}^N_m, \frac{\mathrm{d}}{\mathrm{d}t}\tilde{Z}^N_m\right)_{\omega_\beta,N} = \beta\|\tilde{Z}^N_m\|^2_{\omega_\beta}, \qquad \|\tilde{Z}^N_m\|_{\omega_\beta,N} = \|\tilde{Z}^N_m\|_{\omega_\beta}; \quad (51)$$

by (51) and from the Cauchy inequality, we obtain that

$$\beta\|\tilde{Z}^N_m\|^2_{\omega_\beta} \le 2\|\tilde{Z}^N_m\|_{\omega_\beta,N}\|\frac{\mathrm{d}}{\mathrm{d}t}(\tilde{Z}^N_m)\|_{\omega_\beta,N}, \quad (52)$$

from where

$$\|\tilde{Z}^N_m\|_{\omega_\beta} \le \frac{2}{\beta}\|\frac{\mathrm{d}}{\mathrm{d}t}(\tilde{Z}^N_m)\|_{\omega_\beta}, \quad (53)$$

2. Taking the discrete weighted inner product of (47) with $\tilde{Z}^N_m(t^N_{\beta,k})$, we have

$$\begin{aligned}&\left(\frac{\mathrm{d}}{\mathrm{d}t}\tilde{Z}^N_m + \alpha(t)\tilde{Z}^N_m, \tilde{Z}^N_m\right)_{\omega_\beta,N}\\ &= \left((1+\hbar H)\frac{\mathrm{d}}{\mathrm{d}t}\tilde{Z}^N_{m-1} + \alpha(t)\tilde{Z}^N_{m-1}, \tilde{Z}^N_m\right)_{\omega_\beta,N}\\ &\hbar\left(H(t)[f(t^N_{\beta,k}, Z^N_{m-1} - f(t^N_{\beta,k}, Z^N_{m-2})], \tilde{Z}^N_m\right)_{\omega_\beta,N}\\ &0 \le k \le N, \quad m \ge 1,\end{aligned} \quad (54)$$

Therefore, a combination with Cauchy inequality and (51) leads to

$$\begin{aligned}&\left(\frac{\beta}{2}+\alpha_0\right)\|\tilde{Z}^N_m\|_{\omega_\beta}\\ &\le |1+\hbar H|\|\frac{\mathrm{d}}{\mathrm{d}t}\tilde{Z}^N_{m-1}\|_{\omega_\beta} + \alpha_1||\tilde{Z}^N_{m-1}||_{\omega_\beta}\\ &\quad + |\hbar|H\|f(t^N_{\beta,k}, Z^N_{m-1} - f(t^N_{\beta,k}, Z^N_{m-2})\|_{\omega_\beta,N}.\end{aligned} \quad (55)$$

Then by using inverse inequality of Laguerre polynomial and (48), we get

$$\begin{aligned}&\left(\frac{\beta}{2}+\alpha_0\right)\|\tilde{Z}^N_m\|_{\omega_\beta}\\ &\le (N|1+\hbar H| + \alpha_1 + |\hbar| H L_f)\|\tilde{Z}^N_{m-1}\|_{\omega_\beta},\end{aligned} \quad (56)$$

which is

$$\left\|\tilde{Z}^N_m\right\|_{\omega_\beta} \le \frac{N|1+\hbar H| + \alpha_1 + |\hbar| H L_f}{\beta/2+\alpha_0}\left\|\tilde{Z}^N_{m-1}\right\|_{\omega_\beta} = \gamma\left\|\tilde{Z}^N_{m-1}\right\|_{\omega_\beta}. \quad (57)$$

Hence, we have

$$\left\|\tilde{Z}^N_m\right\|_{\omega_\beta} \le \gamma\left\|\tilde{Z}^N_{m-1}\right\|_{\omega_\beta} \le \cdots \le \gamma^m\left\|\tilde{Z}^N_0\right\|_{\omega_\beta}. \quad (58)$$

Then for any $m' \ge m \ge 1$,

$$\|Z^N_{m'} - Z^N_m\|_{\omega_\beta} \le \sum_{i=m+1}^{m'}\left\|\tilde{Z}^N_i\right\|_{\omega_\beta} \le \sum_{i=m+1}^{m'}\gamma^i\left\|\tilde{Z}^N_0\right\|_{\omega_\beta} \le \frac{\gamma^{m+1}}{1-\gamma}\left\|\tilde{Z}^N_0\right\|_{\omega_\beta}. \quad (59)$$

Since $\gamma \in [0,1)$, $\|Z^N_{m'} - Z^N_m\|_{\omega_\beta} \to 0$ as $m, m' \to \infty$. Thus $\mathscr{Z}_k$ is a Cauchy sequence, and since $\mathbb{R}^n$ is a Banach space, $\mathscr{Z}_k$ has a limit $\hat{Z}(t^N_{\beta,k})$. Taking limit $m \to \infty$ in (43) yields

$$\begin{aligned}\mathcal{L}[\hat{Z}(t^N_{\beta,k}) - \hat{Z}(t^N_{\beta,k})] = 0 = \hbar H(t^N_{\beta,k})\{&\mathcal{L}[\hat{Z}(t^N_{\beta,k})]\\ &+ \mathcal{N}[\hat{Z}(t^N_{\beta,k})] - \phi^N(t^N_{\beta,k})\},\\ \hat{Z}(0) = z^0.&\end{aligned}$$

Thus, $\hat{Z}(t^N_{\beta,k})$ is the exact solution of (17) at any GLR point $t^N_{\beta,k}$. Also, by noticing the definition of $\hat{Z}^N(t)$, it is easy to verify $\hat{Z}^N(t^N_{\beta,k}) = \hat{Z}(t^N_{\beta,k})$, and hence, the proof is completed. ■

5. Numerical experiments

To demonstrate the applicability of the LaHOC algorithm as an appropriate tool for solving infinite horizon optimal control for nonlinear large-scale dynamical systems, we apply the proposed algorithm to several test problems.

Test problem 3.1. Consider the two-order nonlinear composite system described by [7]:

$$\dot{x}_1(t) = x_1(t) + u_1(t) - x_1^3(t) + x_2^2(t), \quad (60)$$

$$\dot{x}_2(t) = -x_2(t) + u_2(t) + x_1(t)x_2(t) + x_2^3(t), \quad (61)$$

$$x_1(0) = 0, \quad x_2(0) = 0.8. \quad (62)$$

The quadratic cost functional to be minimized is given by

$$J = \frac{1}{2}\sum_{i=1}^{2}\int_0^\infty (x_i^2(t) + u_i^2(t))\,dt, \quad (63)$$

In this example, we have $A_1 = B_1 = B_2 = 1$, $A_2 = -1$, $Q_1 = Q_2 = R_1 = R_2 = 1$, $f_1(x) = -x_1^3(t) + x_2^2(t)$, $f_2(x) = x_1(t)x_2(t) + x_2^3(t)$.

Then, according to optimal control theory (3), the optimality conditions can be written as

$$\dot{x}_1(t) = x_1(t) - \lambda_1(t) - x_1^3(t) + x_2^2(t), \quad (64)$$

$$\dot{x}_2(t) = -x_2(t) - \lambda_2(t) + x_1(t)x_2(t) + x_2^3(t), \quad (65)$$

$$\dot{\lambda}_1(t) = -x_1(t) - \lambda_1(t) + 3x_1^2(t)\lambda_1(t) - x_2(t)\lambda_2(t), \quad (66)$$

$$\dot{\lambda}_2(t) = -x_2(t) + \lambda_2(t) - 2x_2(t)\lambda_1(t) - x_1(t)\lambda_2(t) - 3x_2^2(t)\lambda_2(t), \quad (67)$$

$$x_1(0) = 0, \quad x_2(0) = 0.8,$$
$$\lambda_1(\infty) = 0, \quad \lambda_2(\infty) = 0. \quad (68)$$

Also the optimal control laws are $u_1(t) = -\lambda_1$, $u_2(t) = -\lambda_2$.

In this example, the parameters used in the LaHOC algorithms are

$$\mathcal{L}_r = \begin{bmatrix} \frac{d}{dt} - 1 & 0 & 1 & 0 \\ 0 & \frac{d}{dt} + 1 & 0 & 1 \\ 1 & 0 & \frac{d}{dt} + 1 & 0 \\ 0 & 0 & 0 & \frac{d}{dt} - 1 \end{bmatrix},$$

$$\mathbf{A} = \begin{bmatrix} \mathbf{D} - I & O & I & O \\ O & \mathbf{D} + I & O & I \\ I & O & \mathbf{D} + I & O \\ O & O & O & \mathbf{D} - I \end{bmatrix}, \quad (69)$$

$$\mathcal{F}_r = \begin{bmatrix} x_1^3 - x_2^2 \\ -x_1x_2 - x_2^3 \\ -3x_1^2\lambda_1 + x_2\lambda_2 \\ 2x_2\lambda_1 + x_1\lambda_2 + 3x_2^2\lambda_2 \end{bmatrix}, \quad \phi = \begin{bmatrix} 0 \\ 0 \\ 0 \\ 0 \\ 0 \end{bmatrix}, \quad (70)$$

$$R_{r,m-1} = \mathcal{L}_r[x_{r,m-1}] + Q_{r,m-1}, \quad (71)$$

$$Q_{r,m-1} = \begin{bmatrix} -\sum_{j=0}^{m-1} \mathbf{Z}_{1,m-1-j}(t) \sum_{k=0}^{j} \mathbf{Z}_{1,j}(t)\mathbf{Z}_{1,j-k}(t) + \sum_{j=0}^{m-1} \mathbf{Z}_{2,j}\mathbf{Z}_{2,m-1-j} \\ \sum_{j=0}^{m-1} \mathbf{Z}_{1,j}(t)\mathbf{Z}_{2,m-1-j}(t) + \sum_{j=0}^{m-1} \mathbf{Z}_{2,m-1-j}(t) \times \sum_{k=0}^{j} \mathbf{Z}_{2,j}(t)\mathbf{Z}_{2,j-k}(t) \\ 3\sum_{j=0}^{m-1} \mathbf{Z}_{3,m-1-j}(t) \sum_{k=0}^{j} \mathbf{Z}_{1,j}(t)\mathbf{Z}_{1,j-k}(t) - \sum_{j=0}^{m-1} \mathbf{Z}_{2,j}(t)\mathbf{Z}_{4,m-1-j}(t) \\ -2\sum_{j=0}^{m-1} \mathbf{Z}_{2,j}(t)\mathbf{Z}_{3,m-1-j}(t) - \sum_{j=0}^{m-1} \mathbf{Z}_{1,j}(t)\mathbf{Z}_{4,m-1-j}(t) - 3\sum_{j=0}^{m-1} \mathbf{Z}_{4,m-1-j}(t) \times \sum_{k=0}^{j} \mathbf{Z}_{2,j}(t)\mathbf{Z}_{2,j-k}(t) \end{bmatrix}. \quad (72)$$

With these definitions, the LaHOC algorithm gives

$$\mathbf{X}_{r,m} = (\chi_m + \hbar_r)\mathbf{X}_{r,m-1} + \hbar_r\mathbf{A}^{-1}\mathbf{Q}_{r,m-1}. \quad (73)$$

Because the right-hand side of Equation (73) is known, the solution can easily be obtained by using methods for solving a linear system of equations.

Table 1 gives a comparison between the present LaHOC results for $N = 100$ and $\hbar = -0.6$ and the numerically generated BVP5C, at selected values of time t. It can be seen from the table that there is good agreement between the two results. Moreover, our calculations show the better accuracy of LaHOC. In comparison with the BVP5C, it is noteworthy that the LaHOC controls the error bounds while preserving the CPU time. The CPU time of LaHOC is 0.606532 s, and BVP5C is 1.109817 s.

Figure 1 and 2 show the suboptimal states and control for $m = 20$ iterations of LaHOC, compared to MATLAB built-in function BVP5C. The convergence of LaHOC iteration is depicted in Figure 3. Also, Figure 4 presents that the minimum objective functional $|J_j - J_{jj}|$, $j = 1, 2, \ldots, 11$ converges to J_{jj}, where $j = 20 : 10 : 120$ and $jj = 11$.

Table 1. Comparison between the LaHOC solution when $N = 100$ and $\hbar = -0.6$ and BVP4C solution.

	$x_1(t)$		$x_2(t)$		$\lambda_1(t)$		$\lambda_2(t)$	
t	*LaHOC*	*BVP5C*	*LaHOC*	*BVP5C*	*LaHOC*	*BVP5C*	*LaHOC*	*BVP5C*
1	0.000000	0.000000	0.800000	0.800000	0.494159	0.494159	0.766200	0.766189
5	0.002333	0.002333	0.782908	0.782907	0.476481	0.476475	0.729837	0.729804
10	0.010097	0.010098	0.721904	0.721907	0.417587	0.417580	0.612984	0.612940
15	0.020197	0.020198	0.626213	0.626220	0.336861	0.336855	0.464075	0.464028
20	0.028433	0.028436	0.509542	0.509555	0.253927	0.253934	0.325626	0.325617

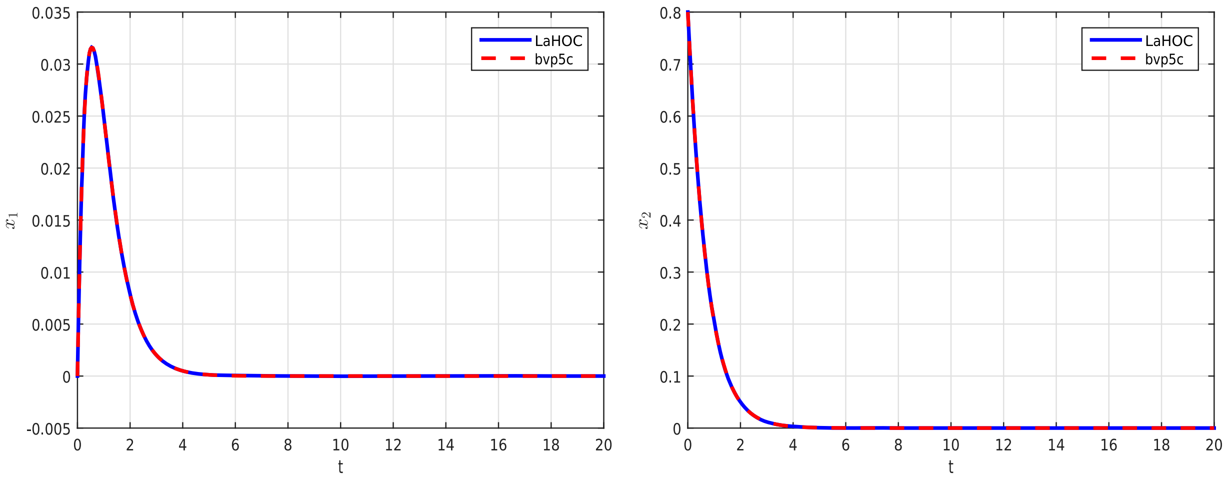

Figure 1. The amplitudes of optimal state variables (Test problem 3.1).

The results obtained with the present method are in good agreement with the results of the successive approximation method used by Tang and Sun [7].

Test problem 3.2. Consider the Euler dynamics and kinematics of a rigid body related to control laws to regulate the attitude of spacecraft and aircraft [7]:

$$\begin{aligned} \dot{\rho}(t) &= \frac{1}{2}(I - S(\rho(t)) + \rho(t)\rho^T(t))\omega(t), \\ \dot{\omega}(t) &= J^{-1}S(\omega(t))J\omega(t) + J^{-1}u(t), \end{aligned} \tag{74}$$

where $J = diag(10, 6.3, 8.5)$, $\rho = (\rho_1, \rho_2, \rho_3)^T \in \mathbb{R}^3$ is the vector of Rodrigues parameters, $\omega = (\omega_1, \omega_2, \omega_3)^T \in \mathbb{R}^3$ is the angular velocity, and $u = (u_1, u_2, u_3)^T \in \mathbb{R}^3$ is the control torque. The symbol $S(\cdot)$ is a skew symmetric matrix of the form

$$S(\omega) = \begin{bmatrix} 0 & \omega_3 & -\omega_2 \\ -\omega_3 & 0 & \omega_1 \\ \omega_2 & -\omega_1 & 0 \end{bmatrix}. \tag{75}$$

In addition, the initial conditions are $\rho(0) = (0.3735, 0.4115, 0.2521)^T$ and $\omega(0) = (0, 0, 0)^T$.

Then, according to optimal control theory (3), the optimality conditions can be written as

$$\begin{aligned} \dot{\rho}_1(t) &= \frac{1}{2}\omega_1(t) + \frac{1}{2}\omega_1(t)\rho_1^2(t) + \frac{1}{2}\omega_2(t)\rho_1(t)\rho_2(t) \\ &\quad + \frac{1}{2}\omega_3(t)\rho_1(t)\rho_3(t), \end{aligned} \tag{76}$$

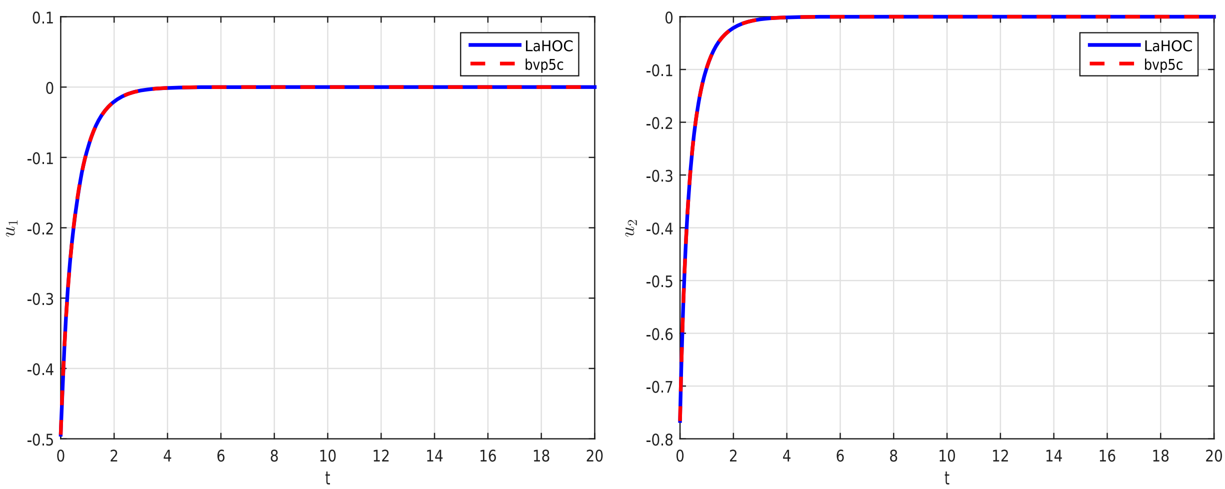

Figure 2. The amplitudes of optimal control variables (Test problem 3.1).

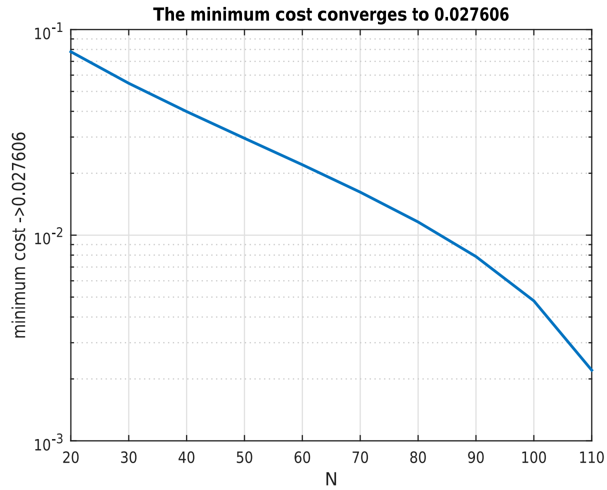

Figure 3. The minimum cost convergence (Test problem 3.1).

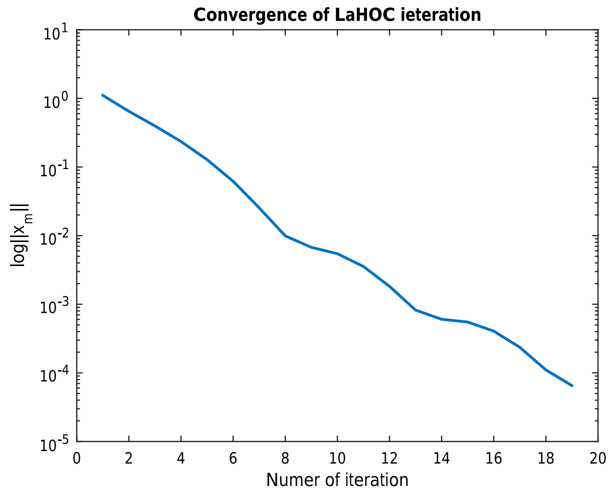

Figure 4. Convergence of LaHOC iteration (Test problem 3.1).

$$\dot{\rho}_2(t) = \frac{1}{2}\omega_2(t) + \frac{1}{2}\omega_2(t)\rho_2^2(t) + \frac{1}{2}\omega_1(t)\rho_1(t)\rho_2(t) + \frac{1}{2}\omega_3(t)\rho_2(t)\rho_3(t), \tag{77}$$

$$\dot{\rho}_3(t) = \frac{1}{2}\omega_3(t) + \frac{1}{2}\omega_3(t)\rho_3^2(t) + \frac{1}{2}\omega_1(t)\rho_1(t)\rho_3(t) + \frac{1}{2}\omega_2(t)\rho_2(t)\rho_3(t), \tag{78}$$

$$\dot{\omega}_1(t) = -\frac{11}{50}\omega_2(t)\omega_3(t) - \frac{1}{100}\lambda_4(t), \tag{79}$$

$$\dot{\omega}_2(t) = -\frac{5}{21}\omega_1(t)\omega_3(t) - \frac{100}{3969}\lambda_5(t), \tag{80}$$

$$\dot{\omega}_3(t) = \frac{37}{85}\omega_1(t)\omega_2(t) - \frac{4}{289}\lambda_6(t), \tag{81}$$

$$\begin{aligned}\dot{\lambda}_1(t) &= -\lambda_1(t)\omega_1(t)\rho_1(t) - \rho_1(t)\\ &\quad - \frac{1}{2}\lambda_1(t)\omega_2(t)\rho_2(t)\\ &\quad - \frac{1}{2}\lambda_1(t)\omega_3(t)\rho_3(t)\\ &\quad - \frac{1}{2}\lambda_2(t)\omega_1(t)\rho_2(t) - \frac{1}{2}\lambda_3(t)\omega_1(t)\rho_3(t),\end{aligned} \tag{82}$$

$$\begin{aligned}\dot{\lambda}_2(t) &= -\lambda_2(t)\omega_2(t)\rho_2(t) - \rho_2(t)\\ &\quad - \frac{1}{2}\lambda_1(t)\omega_2(t)\rho_1(t) - \frac{1}{2}\lambda_2(t)\omega_1(t)\rho_1(t)\\ &\quad - \frac{1}{2}\lambda_2(t)\omega_3(t)\rho_3(t) - \frac{1}{2}\lambda_3(t)\omega_2(t)\rho_3(t),\end{aligned} \tag{83}$$

$$\begin{aligned}\dot{\lambda}_3(t) &= -\lambda_3(t)\omega_3(t)\rho_3(t) - \rho_3(t)\\ &\quad - \frac{1}{2}\lambda_1(t)\omega_3(t)\rho_1(t) - \frac{1}{2}\lambda_2(t)\omega_3(t)\rho_2(t)\\ &\quad - \frac{1}{2}\lambda_3(t)\omega_1(t)\rho_1(t) - \frac{1}{2}\lambda_3(t)\omega_2(t)\rho_2(t),\end{aligned} \tag{84}$$

$$\begin{aligned}\dot{\lambda}_4(t) &= -\frac{37}{85}\lambda_6(t)\omega_2(t) + \frac{5}{21}\lambda_5(t)\omega_3(t)\\ &\quad - \frac{1}{2}\lambda_1(t)\rho_1^2(t) - \frac{1}{2}\lambda_2(t)\rho_1(t)\rho_2(t)\\ &\quad - \frac{1}{2}\lambda_3(t)\rho_1(t)\rho_3(t) - \frac{1}{2}\lambda_1(t) - \omega_1(t),\end{aligned} \tag{85}$$

$$\begin{aligned}\dot{\lambda}_5(t) &= \frac{11}{50}\lambda_4(t)\omega_3(t) - \frac{37}{85}\lambda_6(t)\omega_1(t)\\ &\quad - \frac{1}{2}\lambda_2(t)\rho_2^2(t) - \frac{1}{2}\lambda_1(t)\rho_1(t)\rho_2(t)\\ &\quad - \frac{1}{2}\lambda_3(t)\rho_2(t)\rho_3(t) - \frac{1}{2}\lambda_2(t) - \omega_2(t),\end{aligned} \tag{86}$$

$$\begin{aligned}\dot{\lambda}_6(t) &= -\frac{11}{50}\lambda_4(t)\omega_2(t) + \frac{5}{21}\lambda_5(t)\omega_1(t)\\ &\quad - \frac{1}{2}\lambda_3(t)\rho_3^2(t) - \frac{1}{2}\lambda_1(t)\rho_1(t)\rho_3(t)\\ &\quad - \frac{1}{2}\lambda_2(t)\rho_2(t)\rho_3(t) - \frac{1}{2}\lambda_3(t) - \omega_3(t),\\ \rho_1(0) &= 0.3735, \quad \rho_2(0) = 0.4115, \quad \rho_3(0) = 0.2521,\\ \omega_1(0) &= 0, \quad \omega_2(0) = 0, \quad \omega_3(0) = 0,\end{aligned} \tag{87}$$

and the optimal control laws are $u_1(t) = -\frac{1}{10}\lambda_4$, $u_2(t) = -\frac{10}{63}\lambda_5$, $u_3(t) = -\frac{2}{17}\lambda_6$.

In this example, the parameters used in the LaHOC algorithms are

$$\mathcal{L}_r = \begin{bmatrix} \frac{d}{dt} & 0 & 0 & -\frac{1}{2} & 0 & 0\\ 0 & \frac{d}{dt} & 0 & 0 & -\frac{1}{2} & 0\\ 0 & 0 & \frac{d}{dt} & 0 & 0 & -\frac{1}{2}\\ 0 & 0 & 0 & \frac{d}{dt} & 0 & 0\\ 0 & 0 & 0 & 0 & \frac{d}{dt} & 0\\ 0 & 0 & 0 & 0 & 0 & \frac{d}{dt}\\ 1 & 0 & 0 & 0 & 0 & 0\\ 0 & 1 & 0 & 0 & 0 & 0\\ 0 & 0 & 1 & 0 & 0 & 0\\ 0 & 0 & 0 & 1 & 0 & 0\\ 0 & 0 & 0 & 0 & 1 & 0\\ 0 & 0 & 0 & 0 & 0 & 1 \end{bmatrix}$$

$$\left.\begin{matrix} 0 & 0 & 0 & 0 & 0 & 0 \\ 0 & 0 & 0 & 0 & 0 & 0 \\ 0 & 0 & 0 & 0 & 0 & 0 \\ 0 & 0 & 0 & \frac{1}{100} & 0 & 0 \\ 0 & 0 & 0 & 0 & \frac{100}{3969} & 0 \\ 0 & 0 & 0 & 0 & 0 & \frac{4}{289} \\ \frac{\mathrm{d}}{\mathrm{d}t} & 0 & 0 & 0 & 0 & 0 \\ 0 & \frac{\mathrm{d}}{\mathrm{d}t} & 0 & 0 & 0 & 0 \\ 0 & 0 & \frac{\mathrm{d}}{\mathrm{d}t} & 0 & 0 & 0 \\ \frac{1}{2} & 0 & 0 & \frac{\mathrm{d}}{\mathrm{d}t} & 0 & 0 \\ 0 & \frac{1}{2} & 0 & 0 & \frac{\mathrm{d}}{\mathrm{d}t} & 0 \\ 0 & 0 & \frac{1}{2} & 0 & 0 & \frac{\mathrm{d}}{\mathrm{d}t} \end{matrix}\right], \tag{88}$$

$$\left.\begin{matrix} \mathbf{O} & \mathbf{O} & \mathbf{O} & \mathbf{O} & \mathbf{O} & \mathbf{O} \\ \mathbf{O} & \mathbf{O} & \mathbf{O} & \mathbf{O} & \mathbf{O} & \mathbf{O} \\ \mathbf{O} & \mathbf{O} & \mathbf{O} & \mathbf{O} & \mathbf{O} & \mathbf{O} \\ \mathbf{O} & \mathbf{O} & \mathbf{O} & \frac{1}{100}I & \mathbf{O} & \mathbf{O} \\ \mathbf{O} & \mathbf{O} & \mathbf{O} & \mathbf{O} & \frac{100}{3969}I & \mathbf{O} \\ \mathbf{O} & \mathbf{O} & \mathbf{O} & \mathbf{O} & \mathbf{O} & \frac{4}{289}I \\ \mathbf{D} & \mathbf{O} & \mathbf{O} & \mathbf{O} & \mathbf{O} & \mathbf{O} \\ \mathbf{O} & \mathbf{D} & \mathbf{O} & \mathbf{O} & \mathbf{O} & \mathbf{O} \\ \mathbf{O} & \mathbf{O} & \mathbf{D} & \mathbf{O} & \mathbf{O} & \mathbf{O} \\ \frac{1}{2}I & \mathbf{O} & \mathbf{O} & \mathbf{D} & \mathbf{O} & \mathbf{O} \\ \mathbf{O} & \frac{1}{2}I & \mathbf{O} & \mathbf{O} & \mathbf{D} & \mathbf{O} \\ \mathbf{O} & \mathbf{O} & \frac{1}{2}I & \mathbf{O} & \mathbf{O} & \mathbf{D} \end{matrix}\right], \tag{89}$$

$$\mathbf{A} = \begin{bmatrix} \mathbf{D} & \mathbf{O} & \mathbf{O} & -\frac{1}{2}I & \mathbf{O} & \mathbf{O} \\ \mathbf{O} & \mathbf{D} & \mathbf{O} & \mathbf{O} & -\frac{1}{2}I & I \\ \mathbf{O} & \mathbf{O} & \mathbf{D} & \mathbf{O} & \mathbf{O} & -\frac{1}{2}I \\ \mathbf{O} & \mathbf{O} & \mathbf{O} & \mathbf{D} & \mathbf{O} & \mathbf{O} \\ \mathbf{O} & \mathbf{O} & \mathbf{O} & \mathbf{O} & \mathbf{D} & \mathbf{O} \\ \mathbf{O} & \mathbf{O} & \mathbf{O} & \mathbf{O} & \mathbf{O} & \mathbf{D} \\ I & \mathbf{O} & \mathbf{O} & \mathbf{O} & \mathbf{O} & \mathbf{O} \\ \mathbf{O} & I & \mathbf{O} & \mathbf{O} & \mathbf{O} & \mathbf{O} \\ \mathbf{O} & \mathbf{O} & I & \mathbf{O} & \mathbf{O} & \mathbf{O} \\ \mathbf{O} & \mathbf{O} & \mathbf{O} & I & \mathbf{O} & \mathbf{O} \\ \mathbf{O} & \mathbf{O} & \mathbf{O} & \mathbf{O} & I & \mathbf{O} \\ \mathbf{O} & \mathbf{O} & \mathbf{O} & \mathbf{O} & \mathbf{O} & I \end{bmatrix}$$

$$R_{r,m-1} = \mathcal{L}_r[x_{r,m-1}] + Q_{r,m-1}, \tag{90}$$

$$Q_{r,m-1_{(r=1,2,3)}} = \begin{bmatrix} \frac{1}{2}\sum_{j=0}^{m-1} \mathbf{Z}_{4,m-1-j} \sum_{k=0}^{j} \mathbf{Z}_{1,j}\mathbf{Z}_{1,j-k} \\ \quad + \sum_{j=0}^{m-1} \mathbf{Z}_{5,m-1-j} \sum_{k=0}^{j} \mathbf{Z}_{1,j}\mathbf{Z}_{2,j-k} \\ \quad + \sum_{j=0}^{m-1} \mathbf{Z}_{6,m-1-j} \sum_{k=0}^{j} \mathbf{Z}_{1,j}\mathbf{Z}_{3,j-k}, \\ \frac{1}{2}\sum_{j=0}^{m-1} \mathbf{Z}_{5,m-1-j} \sum_{k=0}^{j} \mathbf{Z}_{2,j}\mathbf{Z}_{2,j-k} \\ \quad + \sum_{j=0}^{m-1} \mathbf{Z}_{4,m-1-j} \sum_{k=0}^{j} \mathbf{Z}_{1,j}\mathbf{Z}_{2,j-k} \\ \quad + \sum_{j=0}^{m-1} \mathbf{Z}_{6,m-1-j} \sum_{k=0}^{j} \mathbf{Z}_{2,j}\mathbf{Z}_{3,j-k}, \\ \frac{1}{2}\sum_{j=0}^{m-1} \mathbf{Z}_{6,m-1-j} \sum_{k=0}^{j} \mathbf{Z}_{3,j}\mathbf{Z}_{3,j-k} \\ \quad + \sum_{j=0}^{m-1} \mathbf{Z}_{4,m-1-j} \sum_{k=0}^{j} \mathbf{Z}_{1,j}\mathbf{Z}_{3,j-k} \\ \quad + \sum_{j=0}^{m-1} \mathbf{Z}_{5,m-1-j} \sum_{k=0}^{j} \mathbf{Z}_{2,j}\mathbf{Z}_{3,j-k}, \end{bmatrix} \tag{91}$$

Table 2. Comparison between the LaHOC solution when $N = 50$ and $\hbar = -1$ and BVP5C solution.

	$\rho_1(t)$		$\rho_2(t)$		$\rho_3(t)$	
t	*LaHOC*	*BVP5C*	*LaHOC*	*BVP5C*	*LaHOC*	*BVP5C*
5	0.374226	0.373454	0.411437	0.411426	0.252506	0.252063
0	0.373694	0.372482	0.409975	0.409878	0.252500	0.251281
15	0.369266	0.368039	0.403332	0.402876	0.251334	0.247714
20	0.358675	0.356639	0.386493	0.385214	0.248508	0.238604
30	0.306469	0.302593	0.309026	0.305203	0.230653	0.196337
40	0.214856	0.209796	0.185840	0.180701	0.186347	0.128007

Table 3. Comparison between the LaHOC solution when $N = 50$ and $\hbar = -1$ and BVP5C solution.

	$\omega_1(t)$		$\omega_2(t)$		$\omega_3(t)$	
t	*LaHOC*	*BVP5C*	*LaHOC*	*BVP5C*	*LaHOC*	*BVP5C*
5	−0.001896	−0.002073	−0.003796	−0.003842	0.000033	−0.001804
10	−0.009180	−0.009462	−0.016999	−0.017336	−0.000362	−0.008219
15	−0.020690	−0.020940	−0.036784	−0.037542	−0.001670	−0.018086
20	−0.034206	−0.034554	−0.058808	−0.059891	−0.004466	−0.029443
30	−0.058410	−0.059101	−0.090380	−0.091566	−0.017421	−0.047287
40	−0.066152	−0.066937	−0.085761	−0.086330	−0.035783	−0.047790

$$Q_{r,m-1} = \begin{bmatrix} -\frac{11}{50}\sum_{j=0}^{m-1}\mathbf{Z}_{5,j}\mathbf{Z}_{6,m-1-j}, \\ -\frac{5}{21}\sum_{j=0}^{m-1}\mathbf{Z}_{4,j}\mathbf{Z}_{6,m-1-j}, \\ \frac{37}{85}\sum_{j=0}^{m-1}\mathbf{Z}_{4,j}\mathbf{Z}_{5,m-1-j}, \\ -\sum_{j=0}^{m-1}\mathbf{Z}_{7,m-1-j}\sum_{k=0}^{j}\mathbf{Z}_{4,j}\mathbf{Z}_{1,j-k} - \frac{1}{2}\sum_{j=0}^{m-1}\mathbf{Z}_{7,m-1-j}\sum_{k=0}^{j}\mathbf{Z}_{5,j}\mathbf{Z}_{2,j-k} - \frac{1}{2}\sum_{j=0}^{m-1}\mathbf{Z}_{7,m-1-j} \\ \sum_{k=0}^{j}\mathbf{Z}_{6,j}\mathbf{Z}_{3,j-k} - \frac{1}{2}\sum_{j=0}^{m-1}\mathbf{Z}_{8,m-1-j}\sum_{k=0}^{j}\mathbf{Z}_{4,j}\mathbf{Z}_{2,j-k} - \frac{1}{2}\sum_{j=0}^{m-1}\mathbf{Z}_{9,m-1-j}\sum_{k=0}^{j}\mathbf{Z}_{4,j}\mathbf{Z}_{3,j-k}, \\ -\sum_{j=0}^{m-1}\mathbf{Z}_{8,m-1-j}\sum_{k=0}^{j}\mathbf{Z}_{5,j}\mathbf{Z}_{2,j-k} - \frac{1}{2}\sum_{j=0}^{m-1}\mathbf{Z}_{7,m-1-j}\sum_{k=0}^{j}\mathbf{Z}_{5,j}\mathbf{Z}_{1,j-k} - \frac{1}{2}\sum_{j=0}^{m-1}\mathbf{Z}_{8,m-1-j} \\ \sum_{k=0}^{j}\mathbf{Z}_{4,j}\mathbf{Z}_{1,j-k} - \frac{1}{2}\sum_{j=0}^{m-1}\mathbf{Z}_{8,m-1-j}\sum_{k=0}^{j}\mathbf{Z}_{6,j}\mathbf{Z}_{3,j-k} - \frac{1}{2}\sum_{j=0}^{m-1}\mathbf{Z}_{8,m-1-j}\sum_{k=0}^{j}\mathbf{Z}_{5,j}\mathbf{Z}_{3,j-k}, \\ -\sum_{j=0}^{m-1}\mathbf{Z}_{9,m-1-j}\sum_{k=0}^{j}\mathbf{Z}_{6,j}\mathbf{Z}_{3,j-k} - \frac{1}{2}\sum_{j=0}^{m-1}\mathbf{Z}_{7,m-1-j}\sum_{k=0}^{j}\mathbf{Z}_{6,j}\mathbf{Z}_{1,j-k} - \frac{1}{2}\sum_{j=0}^{m-1}\mathbf{Z}_{8,m-1-j} \\ \sum_{k=0}^{j}\mathbf{Z}_{6,j}\mathbf{Z}_{2,j-k} - \frac{1}{2}\sum_{j=0}^{m-1}\mathbf{Z}_{9,m-1-j}\sum_{k=0}^{j}\mathbf{Z}_{4,j}\mathbf{Z}_{1,j-k} - \frac{1}{2}\sum_{j=0}^{m-1}\mathbf{Z}_{9,m-1-j}\sum_{k=0}^{j}\mathbf{Z}_{5,j}\mathbf{Z}_{2,j-k}, \\ -\frac{37}{85}\sum_{j=0}^{m-1}\mathbf{Z}_{12,j}\mathbf{Z}_{5,m-1-j} + \frac{5}{21}\sum_{j=0}^{m-1}\mathbf{Z}_{11,j}\mathbf{Z}_{6,m-1-j} - \frac{1}{2}\sum_{j=0}^{m-1}\mathbf{Z}_{7,m-1-j}\sum_{k=0}^{j}\mathbf{Z}_{1,j}\mathbf{Z}_{1,j-k} \\ -\frac{1}{2}\sum_{j=0}^{m-1}\mathbf{Z}_{8,m-1-j}\sum_{k=0}^{j}\mathbf{Z}_{1,j}\mathbf{Z}_{2,j-k} - \frac{1}{2}\sum_{j=0}^{m-1}\mathbf{Z}_{9,m-1-j}\sum_{k=0}^{j}\mathbf{Z}_{1,j}\mathbf{Z}_{3,j-k}, \\ \frac{11}{50}\sum_{j=0}^{m-1}\mathbf{Z}_{10,j}\mathbf{Z}_{6,m-1-j} - \frac{37}{85}\sum_{j=0}^{m-1}\mathbf{Z}_{12,j}\mathbf{Z}_{4,m-1-j} - \frac{1}{2}\sum_{j=0}^{m-1}\mathbf{Z}_{8,m-1-j}\sum_{k=0}^{j}\mathbf{Z}_{2,j}\mathbf{Z}_{2,j-k} \\ -\frac{1}{2}\sum_{j=0}^{m-1}\mathbf{Z}_{7,m-1-j}\sum_{k=0}^{j}\mathbf{Z}_{1,j}\mathbf{Z}_{2,j-k} - \frac{1}{2}\sum_{j=0}^{m-1}\mathbf{Z}_{9,m-1-j}\sum_{k=0}^{j}\mathbf{Z}_{2,j}\mathbf{Z}_{3,j-k}, \\ -\frac{11}{50}\sum_{j=0}^{m-1}\mathbf{Z}_{10,j}\mathbf{Z}_{5,m-1-j} + \frac{5}{21}\sum_{j=0}^{m-1}\mathbf{Z}_{11,j}\mathbf{Z}_{4,m-1-j} - \frac{1}{2}\sum_{j=0}^{m-1}\mathbf{Z}_{9,m-1-j}\sum_{k=0}^{j}\mathbf{Z}_{3,j}\mathbf{Z}_{3,j-k} \\ -\frac{1}{2}\sum_{j=0}^{m-1}\mathbf{Z}_{7,m-1-j}\sum_{k=0}^{j}\mathbf{Z}_{1,j}\mathbf{Z}_{3,j-k} - \frac{1}{2}\sum_{j=0}^{m-1}\mathbf{Z}_{8,m-1-j}\sum_{k=0}^{j}\mathbf{Z}_{2,j}\mathbf{Z}_{3,j-k} \end{bmatrix}.$$

With these definitions, the LaHOC algorithm gives

$$\mathbf{X}_{r,m} = (\chi_m + \hbar_r)\mathbf{X}_{r,m-1} + \hbar_r\mathbf{A}^{-1}\mathbf{Q}_{r,m-1}. \quad (92)$$

Because the right-hand side of Equation (92) is known, the solution can easily be obtained by using methods for solving linear systems of equations.

Tables 2 and 3 give a comparison between the present *SHAM* results for $N = 50$ and $\hbar = -1$ and the numerically generated BVP5C at selected values of time t. It can be seen from the tables that there is good agreement between the two results. Moreover, our calculations show the better accuracy of LaHOC. In comparison with the BVP5C, it is noteworthy that the LaHOC controls the error bounds while preserving the CPU time. The CPU time of LaHOC is 1.009860 s, and BVP5C is 4.514071 s.

Figures 5–9 show the suboptimal states and control for $m = 20$ iterations of LaHOC compared to MATLAB the built-in function BVP5C. The convergence of the LaHOC iteration is depicted in Figure 10.

The obtained optimal trajectories and optimal controls are identical to those obtained by Jajarmi et al. [8].

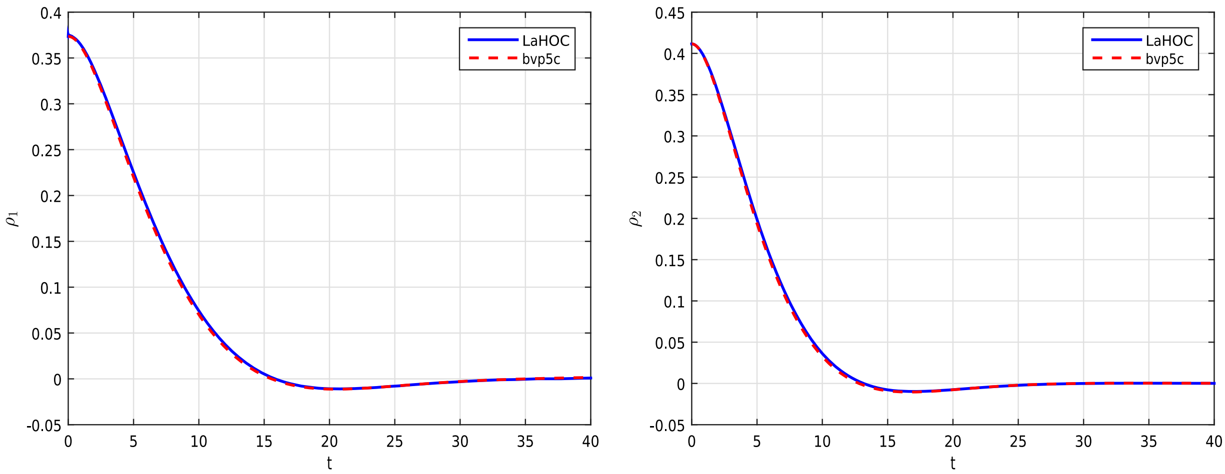

Figure 5. The amplitudes of optimal state variables of ρ_1, ρ_2 (Test problem 3.2).

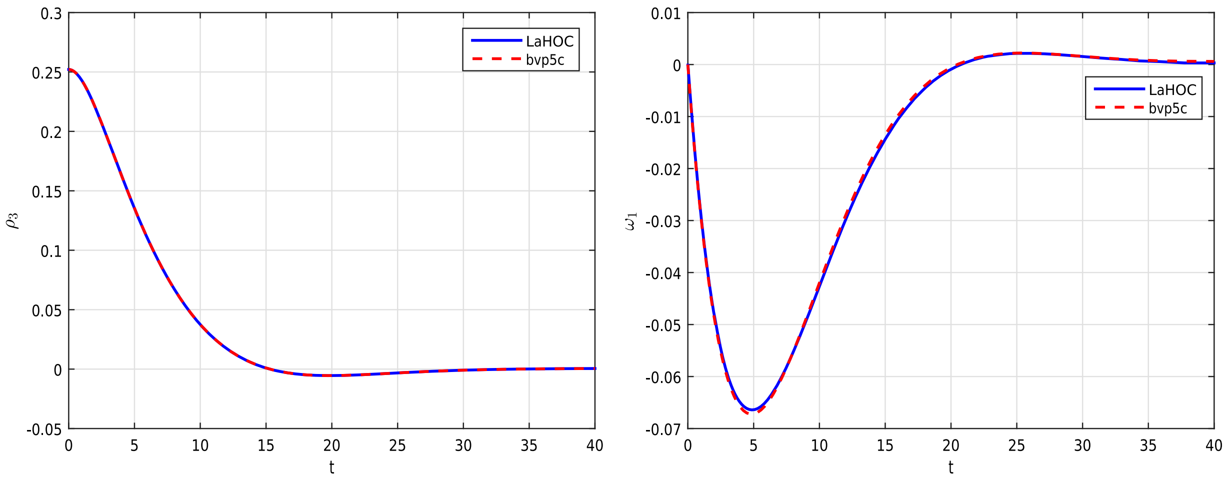

Figure 6. The amplitudes of optimal state variables of ρ_3, ω_1 (Test problem 3.2).

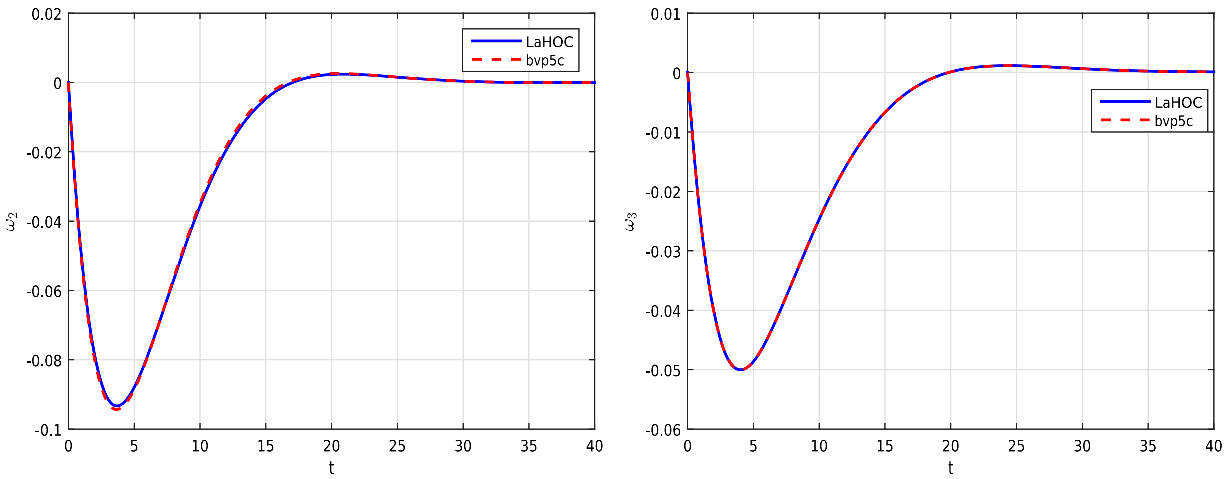

Figure 7. The amplitudes of optimal state variables of ω_2, ω_3 (Test problem 3.2).

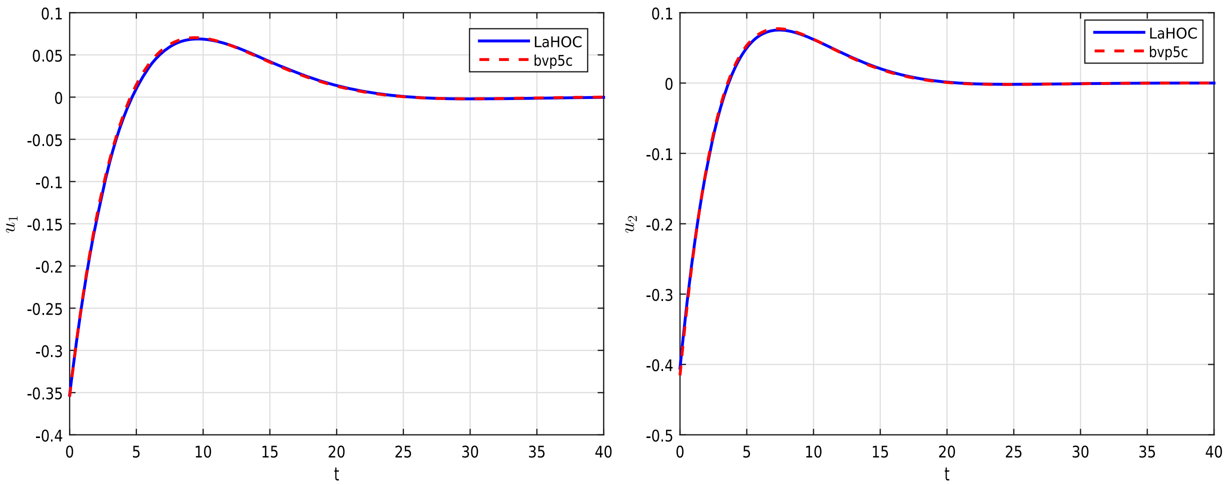

Figure 8. The amplitudes of optimal control variables u_1, u_2 (Test problem 3.2).

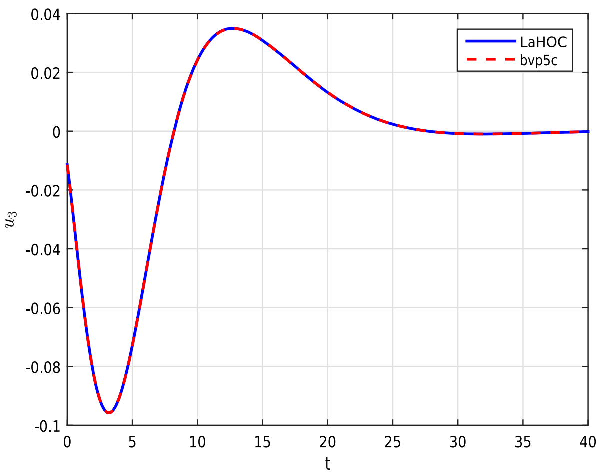

Figure 9. The amplitudes of optimal control variable u_3 (Test problem 3.2).

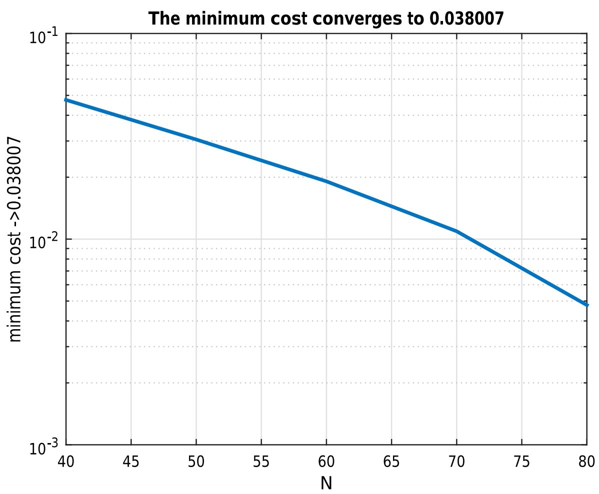

Figure 10. The minimum cost convergence (Test problem 3.2).

6. Conclusion

In this paper, an effective method based upon the spectral homotopy method with Laguerre basis (LaHOC) is proposed for finding the numerical solutions of the infinite horizon optimal control problem of nonlinear interconnected large-scale dynamic systems. A modified Laguerre method is used to discretize the equation of optimal condition, while a homotopy method is used to construct an iterative scheme. Two illustrative examples demonstrated that LaHOC has spectral accuracy and very good efficiency, which is comparable to well-established numerical methods such as the MATLAB BVP5C solver. The second example shows when the multi-components have different time and amplitude scales, one need to use adaptive rescaling technique in the Laguerre bases to improve accuracy, which deserves a further study.

Disclosure statement

No potential conflict of interest was reported by the author(s).

ORCID

Hassan Saberi Nik http://orcid.org/0000-0003-2521-1325

References

[1] Jamshidi M. Large-scale systems: modeling and control. New York (NY): North-Holland; 1983.
[2] Haddad WM, Nersesov SG. Stability and control of large-scale dynamical systems. A Vector Dissipative Systems approach. Princeton (NJ): Princeton University Press; 2011.
[3] Holland C, Diamond PH. On the dynamics of large-scale structures in electron temperature gradient turbulence. Phys Lett A. 2005;344(5):369–382.
[4] Huang SN, Tan KK, Lee TH. Decentralized control of a class of large scale nonlinear systems using neural networks. Automatica. 2005;41(9):1645–1649.
[5] Chen W, Li J. Decentralized output feedback neural control for systems with unknown interconnections. IEEE Trans Syst Man Cybern Part B. 2008;38(1):258–266.
[6] Yan XG, Lam J, Dai GZ. Decentralized robust control for nonlinear large-scale systems with similarity. Comput Electr Eng. 1999;25(3):169–179.
[7] Tang GY, Sun L. Optimal control for nonlinear interconnected large-scale systems: a successive approximation approach. Acta Automat Sinica. 2005;31(2):248–254.

[8] Jajarmi A, Pariz N, Effati S, et al. Infinite horizon optimal control for nonlinear interconnected large-scale dynamical systems with an application to optimal attitude control. Asian J Control. 2013;15(6):1–12.

[9] Chang I, Park SY, Choi KH. Decentralized coordinated attitude control for satellite formation flying via the state-dependent Riccati equation technique. Int J Nonlinear Mech. 2009;44(8):891–904.

[10] Rafiei Z, Kafash B, Karbassi SM. A new approach based on using Chebyshev wavelets for solving various optimal control problems. Comput Appl Math. 2017. doi:10.1007/s40314-017-0419-z.

[11] Ross IM, Fahroo F. Legendre pseudo-spectral approximations of optimal control problems. In: Kang W, Borges C, Xiao M, editors. New trends in nonlinear dynamics and control and their applications. Lecture notes in control and information science. Berlin: Springer; 2004. p. 327–342.

[12] Ross IM, Fahroo F. Pseudospectral knotting methods for solving nonsmooth optimal control problems. J Guid Control Dyn. 2004;27(3):397–405.

[13] Tang T. The Hermite spectral method for Gaussian-type functions. SIAM J Sci Comput. 1993;14:594594.

[14] Guo BY, Wang ZQ, Tian HJ, et al. Integration processes of ordinary differential equations based on Laguerre-Radau interpolations. Math Comput. 2008;77(261):181–199.

[15] Shen J, Wang LL. Some recent advances on spectral methods for unbounded domains. Commun Comput Phys. 2009;5(2–4):195–241.

[16] Shen J, Yu HJ. Efficient spectral sparse grid methods and applications to high-dimensional elliptic equations II. Unbounded domains. SIAM J Sci Comput. 2012;34(2):1141–1164.

[17] Shen J, Wang LL, Yu HJ. Approximations by orthonormal mapped Chebyshev functions for higher-dimensional problems in unbounded domains. J Comput Appl Math. 2014;265:264–275.

[18] Wan X, Yu HJ. A dynamic-solver-consistent minimum action method: with an application to 2D Navier-Stokes equations. J Comput Phys. 2017;331:209–226.

[19] Liao SJ. On the homotopy analysis method for nonlinear problems. Appl Math Comput. 2004;147:499–513.

[20] Liao SJ. Beyond perturbation: introduction to homotopy analysis method. Boca Raton: Chapman & Hall/CRC Press; 2003.

[21] Xu D, Cui J, Liao S, et al. A HAM-based analytic approach for physical models with an infinite number of singularities. Numer Algorithms. 2014. doi:10.1007/s11075-014-9881-5

[22] Abbasbandy S, Shirzadi A. A new application of the homotopy analysis method: solving the Sturm-Liouville problems. Commun Nonlinear Sci Numer Simul. 2011;16:112–126.

[23] Abbasbandy S, Shirzadi A. Homotopy analysis method for multiple solutions of the fractional Sturm-Liouville problems. Numer Algorithms. 2010;54:521–532.

[24] Effati S, Saberi Nik H, Shirazian M. Analytic-approximate solution for a class of nonlinear optimal control problems by homotopy analysis method. Asian-Euro J Math. 2013;6(2):1350012.

[25] Jajarmi A, Dehghan Nayyeri M, Saberi Nik H. A novel feedforward-feedback suboptimal control of linear time-delay systems. J Complexity. 2016;35:46–62.

[26] Van Gorder RA. Control of error in the homotopy analysis of semi-linear elliptic boundary value problems. Numer Algorithms. 2012;61(4):613–629.

[27] Baxter M, Van Gorder RA, Vajravelu K. On the choice of auxiliary linear operator in the optimal homotopy analysis of the Cahn-Hilliard initial value problem. Numer Algorithms. 2014;66(2):269–298.

[28] Zhu Z, Yu B. A modified homotopy method for solving the principal-agent bilevel programming problem. Comput Appl Math. 2016. doi:10.1007/s40314-016-0361-5

[29] Motsa SS, Sibanda P, Shateyi S. A new spectral-homotopy analysis method for solving a nonlinear second order BVP. Commun Nonlinear Sci Numer Simul. 2010;15:2293–2302.

[30] Motsa SS, Sibanda P, Awad FG, et al. A new spectral-homotopy analysis method for the MHD Jeffery-Hamel problem. Comput Fluids. 2010;39:1219–1225.

[31] Moghtadaei M, Saberi Nik H, Abbasbandy S. A spectral method for the electrohydrodynamic flow in a circular cylindrical conduit. Chin Ann Math. 2015;36B(2):307–322.

[32] Saberi Nik H, Effati S, Motsa SS, et al. Spectral homotopy analysis method and its convergence for solving a class of nonlinear optimal control problems. Numer Algorithms. 2014;65:171–194.

[33] Shen J, Tang T, Wang LL. Spectral methods algorithms, analysis and applications. Springer series in computational mathematics, vol. 41. Berlin: Springer-Verlag; 2011.

[34] Saadatmandi A, Akbari Z. Transformed Hermite functions on a finite interval and their applications to a class of singular boundary value problems. Comput Appl Math. 2015;00:1–14.

[35] Doha EH, Bhrawy AH, Hafez RM, et al. A Jacobi rational pseudospectral method for Lane-Emden initial value problems arising in astrophysics on a semi-infinite interval. Comput Appl Math. 2014;33-3:607–619.